IEEE Access
Multidisciplinary | Rapid Review | Open Access Journal

Received September 17, 2019, accepted October 6, 2019, date of publication October 22, 2019, date of current version November 21, 2019.

Digital Object Identifier 10.1109/ACCESS.2019.2948822

Heterogeneous UAV Cells: An Effective Resource Allocation Scheme for Maximum Coverage Performance

NIMA NAMVAR[1], (Student Member, IEEE), ABDOLLAH HOMAIFAR[1], ALI KARIMODDINI[1], AND BEHROUZ MAHAM[2], (Senior Member, IEEE)

[1]Autonomous Control and Information Technology Institute, North Carolina A&T State University, Greensboro, NC 27411, USA
[2]Department of Electrical and Computer Engineering, Nazarbayev University, Astana 010000 , Kazakhstan

Corresponding author: Abdollah Homaifar (homaifar@ncat.edu)

This work was supported by the Air Force Research Laboratory and OSD for sponsoring this research under Grant FA8750-15-2-0116.

ABSTRACT This paper develops an effective approach for the 3D deployment of a heterogeneous set of unmanned aerial vehicles (UAVs) acting as aerial base stations that provide maximum wireless coverage for ground users in a given geographical area. This problem is addressed in two steps. First, in order to maximize the utilization of each UAV, its optimal flight altitude is found based on the UAV's transmit power which provides maximum coverage radius on the ground. The UAVs are classified into separate groups based on their transmit powers and optimal flight altitudes. Next, given a repository of UAVs belonging to different classes, the proposed technique finds an optimal subset of the available UAVs along with their optimal 3D placement to provide the maximum network coverage for a given area on the ground with the minimum power consumption. This optimization problem is proved to be NP-hard, for which a novel algorithm is proposed to solve the problem. Simulation results demonstrate the effectiveness of the proposed solution and provide valuable insights into the performance of the Heterogeneous UAV-supported small cell networks.

INDEX TERMS Unmanned aerial vehicle (UAV), heterogeneous UAV base stations (UAV-BSs), coverage maximization, constrained circle packing.

I. INTRODUCTION

A. MOTIVATION

Recent years have witnessed increasingly more exercises and usages of Unmanned Aerial Vehicles (UAVs), such as drones and balloons for boosting the capacity and enhancing the wireless coverage of terrestrial networks [1]. Indeed, with advances in wireless networking technologies, UAVs can be equipped with wireless transceivers which enable them to communicate with ground devices as well as other UAVs. Hence, UAVs can serve as flying base stations (BSs) to form an ad-hoc network and provide on-demand wireless coverage in a given geographical area [2]. This is particularly useful where the cellular network is either unavailable or needs to be assisted to provide the required capacity and coverage. For example, Verizon has developed airborne LTE service for delivering 4G-LTE service in ''coverage-denied environments'' during an emergency management and disaster recovery exercise [3]. Moreover, the Aquila project by Facebook [4] and the Loon project by Google [5] leverage the UAV technology to create an aerial wireless network which provides ubiquitous internet access to rural and remote areas up to 4G-LTE speeds. In fact, by virtue of their inherent attributes such as flexibility, mobility, and higher altitude, UAVs have a higher chance of establishing line-of-sight (LoS) communication links for ground users [6]. This is particularly useful in situations where the ground nodes are scattered or obstacles such as hills and large man-made structures deteriorate the quality of links over ground-to-ground communications. Thanks to such advantages, UAVs are being increasingly utilized by wireless carriers such as AT&T to enhance wireless coverage in hot spots such as big concerts and stadiums where the cellular network is over congested and needs further assistance to maintain its service level [7].

Wireless networking with UAVs faces a number of technical challenges that are substantially different with the conventional terrestrial networks. The key features that distinguish UAV-based communication from conventional wireless networks include: a) dependency of coverage performance on

The associate editor coordinating the review of this manuscript and approving it for publication was Xujie Li.

the LoS propagation and elevation angle, b) highly dynamic channels due to the mobility of both the aerial base station and the ground operators, and c) airframe shadowing caused by the structural design and rotation of the UAV [8]. The major design problems in UAV communication include 3D deployment of the UAVs, energy efficiency, resource allocation, and cell association.

Recent studies on UAV communications have investigated various design challenges, such as the air-to-ground (ATG) transmission model [9]–[11], UAV deployment/placement optimization, and various applications across different domains [12]–[17]. In particular, the deployment problem is of significant importance because it directly affects the total coverage area, energy consumption, and the interference generated by the UAV-BSs. In this paper, we aim to address the effective deployment of a set of heterogeneous UAVs with various transmit power and coverage radii acting as aerial quasi-static BSs to maximize the coverage area while taking into account the total energy consumption by the UAVs.

B. RELATED WORKS AND OUR CONTRIBUTION

Majority of the existing work on UAV communications is devoted to the ATG channel modeling. For instance, the authors in [9] provided a statistical generic ATG propagation model for Low Altitude Platform (LAP) systems in which the probability of LoS channel is derived as a function of the elevation angle. The work in [10] studies the effects of shadowing and pathloss for UAV communications in dense urban environments. As discussed in [11], due to the pathloss and shadowing, the characteristics of the ATG channel depend on the height of the aerial base stations. A comprehensive survey on available ATG propagation models can be found in [18].

To address the UAV deployment challenge, the authors in [19] provide an analytical approach to optimize the altitude of a single UAV for providing maximum coverage area on the ground. In [20], a UAV-enabled small cell placement optimization problem is investigated in the presence of a terrestrial wireless network to maximize the number of users that can be covered. The optimal flight altitude of a single UAV-BS operating under the Rician fading channel is derived in [21]. Despite providing valuable insight into UAV communications, the works presented so far are limited by considering only a single UAV. The problem of multiple UAV deployment is much more challenging as the the distance between the UAV-BSs and their relative positions affects the overall coverage performance. Moreover, due to the presence of interference between the received signal from different UAVs, additional interference management/avoidance protocols are necessary.

The authors in [22] proposed a novel energy-efficient rechargeable UAV deployment strategy to provide seamless connectivity in urban areas. The work in [23] investigated the coverage of two UAV-BSs positioned at a fixed altitude and study the effect of inter-cell interference on the total coverage. The authors in [24] studied the use of multiple UAVs as wireless relays in order to facilitate the communication between ground sensor nodes. However, the work in [24] does not consider the use of UAVs as aerial BSs. In [25], a method for the positioning of identical UAV-BSs in wireless temporary networks is proposed in which the overlapping coverage areas by different UAVs is allowed which necessitates the use of inter-cell interference coordination (ICIC). The work in [26] provides a framework for throughput analysis in a multi-UAV enabled wireless network assuming that the UAVs hover at the same altitude and share the same frequency band. The authors then proposed a power control method to mitigate the co-channel interference for the ground users. Assuming a fixed flight altitude for the UAVs, the horizontal 2D positions of UAVs are optimized in [27] to minimize the number of required UAV-BSs to cover a given set of ground users. The optimal placement of multiple symmetric UAVs with the assumption of having the same transmit power and altitude is further studied in [28].

Most existing results on multiple UAV deployment, as discussed above, consider the scenario of implementing identical or symmetrical UAVs in which the UAVs either have the same altitude or same transmit power. Moreover, the number of UAVs to be deployed in a given area is assumed to be known in advance. In practice, however, one might have a repository of various types of UAVs with different capabilities which are to be deployed in a given area to provide wireless coverage. In this context, the exact number and the type of UAVs that need to be deployed depend on the target area. For example, having a large set of UAVs, one may need to use only a few UAVs in order to cover a small area of interest. Otherwise, the efficiency of resource allocation may drop significantly due to over allocation of resources, i.e., UAV-BSs. Moreover, such over allocation of resources may lead to excessive interference between the UAVs, which in turn, deteriorates the overall quality of service (QoS).

The main contribution of this paper is to develop an efficient technique for deployment of a heterogeneous set of UAVs to provide maximum network coverage for an area of interest. In particular, given a set of heterogeneous UAVs with various transmit power, we propose an efficient algorithm for 3D placement of the UAVs as aerial quasi-static BSs in order to maximize the wireless coverage in a given area. The advantage of the proposed method is that rather than deploying all available UAVs, we use as many UAVs as are needed to provide network coverage while maintaining the desired quality of service (QoS). In this way, the number and the type of UAVs are design factors to be determined based on the size and shape of the area of interest. To develop the proposed technique, we first capture the characteristics of the ATG channel. Next, in order to utilize the maximum potential of the UAVs, we find the optimal flight altitude for each UAV as a function of its transmit power and environmental factors. We then determine the minimum number of UAVs and their optimal placement to provide maximum coverage, while minimally utilizing the available resources (total UAV power transmit) and avoiding inter-cell interference to reduce the

network overhead. Due to the complexity of this optimization problem, a closed form solution cannot be found. In order to solve this problem, we propose a novel evolutionary algorithm which, given the coverage radii of the available UAVs in the repository, determines the type, number, and horizontal position of UAVs to be deployed in order to maximize the total coverage. The simulation results are provided to demonstrate the effectiveness of the proposed method.

The rest of this paper is organized as follows. Section II presents the system model and describes the air-to-ground channel model. The optimal flight altitude of each UAV is derived in Section III. Section IV formulates an optimization problem which simultaneously determines the optimal resource allocation strategy, i.e., selection of the UAVs, and the optimal horizontal position of the UAVs for maximum wireless coverage. Section V presents the proposed algorithm for optimal selection and horizontal placement of UAVs. Simulation results are provided in Section VI while Section VII draws some conclusions.

II. SYSTEM MODEL

Consider a heterogeneous repository of UAVs in which the UAVs are of various types depending on their transmit power. Let $\mathcal{U} = \{U_i\}_{i=1}^{N}$ denote the set of N available UAVs in the repository while P_i^t represent the transmit power of UAV U_i. Considering a 2D geographical area located in an urban environment, our aim is to allocate available resources, i.e., the UAVs, to provide wireless coverage over the area of interest. The type and number of UAVs to be deployed depends on the size and shape of the area that needs to be covered. Without loss of generality, consider the area of interest to be a rectangular area with the length L and width W as shown in Figure 1. In this paper, we consider a quasi-stationary low altitude platform (LAP) such as quadrotor UAVs. Note that although the LAP is stationary, the UAVs can hover at different altitudes to achieve their maximum possible coverage radius according to their transmit power. In this regard, we seek to optimize the location of the UAV-supported cells in order to provide maximum coverage with minimum energy consumption using the available UAVs in the repository.

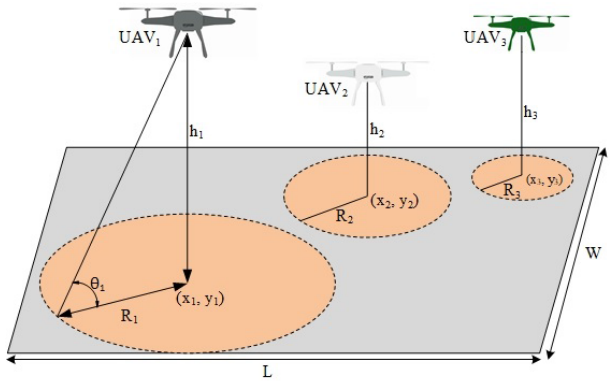

FIGURE 1. System Model: a set of heterogeneous UAVs provide wireless coverage in a rectangular area with length L and width W. The UAVs hover at different altitudes, depending on their transmit power and environmental factors.

In order to analyze the wireless coverage of the UAVs, we first study the ATG channel propagation model. The ATG propagation model is substantially different from the terrestrial propagation model as it posses a higher chance of line-of-sight (LoS) connectivity. As discussed in [9] and [19], the radio signal from a LAP base station (LAP-BS) reaches its destination in accordance to two main propagation groups. The first group corresponds to receiving a LoS signal while the second group corresponds to receiving a strong non-LoS (NLoS) signal due to reflections and diffractions. These groups can be considered separately with different probabilities of occurrence which depend on the environmental factors such as the density and height of buildings, and the elevation angle. In this work, we adopt the model presented in [19] for characterizing the ATG channels for LAP systems.

Radio signals emitted by a LAP-BS propagate in free space until reaching the ground receivers. The main attenuation that a LAP signal incurs is the free space pathloss (FSPL) which is given by:

$$\text{FSPL} = 20\log\left(\frac{4\pi f_c d}{c}\right), \tag{1}$$

in which f_c is the carrier frequency and c is the speed of light. In addition, $d = \sqrt{h^2 + r^2}$ is the distance between the UAV hovering at altitude h and the ground receiver located at radial distance r from the UAV in the 2D plane as shown in Figure 1.

Apart from FSPL, the radio signals emitted by a LAP-BS incur additional loss due to shadowing and scattering, which is caused by the obstacles in the environment and can be best modeled as a Lognormal distribution [19]. In this work, we use the mean value of LoS rather than its instantaneous characteristics as the planning for deployment of stationary LAP-BSs should be done based on the expected and long term variations of the channel. The total mean pathloss model for ATG channel is therefore given by

$$PL(\text{dB}) = \text{FSPL}(\text{dB}) + \eta_\xi(\text{dB}), \tag{2}$$

where η_ξ represents the excessive pathloss due to shadowing and scattering in which the subscript ξ refers to the propagation group such that $\eta_\xi \in \{\eta_{LoS}, \eta_{NLoS}\}$. Each propagation group happens with a specific probability which depends on the environment. The values of η_{LoS} and η_{NLoS} should be found experimentally and η_{NLoS} is typically much larger than η_{LoS} [9]. black As the excessive pathloss, η_ξ, takes on two values, i.e., η_{LoS} and η_{NLoS} with probabilities P_{LoS} and $P_{\text{NLoS}} = 1 - P_{\text{LoS}}$, it can be modeled as a Bernoulli random variable with parameter $\mathbf{P}_{\text{LoS}}$ as given in [9],

$$\eta_\xi \sim \text{Bernoulli}\left(\mathbf{P}_{\text{LoS}}\right), \tag{3}$$

where $\mathbf{P}_{\text{LoS}}$ is the probability of having a LoS link and $\mathbf{P}_{\text{NLoS}} = 1 - \mathbf{P}_{\text{LoS}}$ is the probability of having a NLoS link. As shown in [9], the probability of receiving LoS signal from UAV-BS U_i for a ground user located at (X, Y) depends on the altitude of the UAV-BS, h_i, and its horizontal distance to the

user that is equal to $r_i = \sqrt{(X - x_i)^2 + (Y - y_i)^2}$, in which (x_i, y_i) is the location of the UAV-BS at the 2D plane. The LoS probability is given by [9]:

$$\mathbf{P}_{\text{LoS}}(h_i, r_i) = \frac{1}{1 + \alpha \exp\big(-\beta(\arctan\big(\frac{h_i}{r_i}\big) - \alpha)\big)}, \quad (4)$$

in which α and β are constant values which depend on the environment. Since we cannot determine whether the link is LoS or NLoS as a priori, we consider the spatial expectation of the pathloss over LoS and NLoS links,

$$\overline{PL}(\text{dB}) = \text{FSPL}(\text{dB}) + \eta_{\text{LoS}}(\text{dB})\mathbf{P}_{\text{LoS}} + \eta_{\text{NLoS}}(\text{dB})\mathbf{P}_{\text{NLoS}}. \quad (5)$$

By substituting (1) and (4) into (5), and letting $d_i = \sqrt{h_i^2 + r_i^2}$ to be the distance between the UAV U_i and the user, we have

$$\overline{PL}(\text{dB}) = 20\log(d_i) + \frac{A}{1 + \alpha \exp(-\beta(\theta - \alpha))} + B, \quad (6)$$

in which $A = \eta_{\text{LoS}}(\text{dB}) - \eta_{\text{NLoS}}(\text{dB})$ and $B = \eta_{\text{NLoS}}(\text{dB}) + 20\log(\frac{4\pi f_c}{c})$.

III. OPTIMAL FLIGHT ALTITUDE FOR MAXIMUM UTILIZATION OF DEPLOYED UAVS

Despite the conventional terrestrial BSs, the coverage radii of the UAV-BSs are not known in advance and depend on their altitude. Therefore, in order to utilize the maximum potential of the UAVs, here we obtain the optimal flight altitude for each UAV which results in the largest coverage radius on the ground. More specifically, given a UAV-BS $U_i \in \mathcal{U}$ with transmit power P_i^t, we find its optimal flight altitude h_i, which maximizes the size of the covered area. We define the service threshold in terms of the minimum allowable received signal power for a successful transmission. Any point in the area is covered if its received signal power is greater than a threshold ϵ.

Remark 1: As it is presented in the Section IV, the coverage areas of the UAVs do not overlap and thus, there is no inter-cell interference among the UAV-BSs. Consequently, using the signal-to-noise (SNR) measure for defining the service threshold is equivalent to the signal-to-noise-plus-interference (SINR) criterion.

Having defined the expected pathloss in (6), the received signal power at a ground receiver located in radial distance r_i from the ground image of the UAV is given by

$$P^r(\text{dB}) = P_i^t(\text{dB}) - \overline{PL}(\text{dB}), \quad (7)$$

which requires to be greater than ϵ, i.e., $P^r \geq \epsilon$. This is equivalent to having

$$\overline{PL}(\text{dB}) \leq P_i^t(\text{dB}) - \epsilon. \quad (8)$$

Proposition 1: The coverage area of a UAV-BS with transmit power $P_i^t(dB)$ hovering at a fixed altitude h_i is a circular disk.

Proof: According to the equation (8), for a given transmit power $P_i^t(\text{dB})$, the wireless coverage for a ground point only depends on the average pathloss $\overline{PL}(\text{dB})$ which is experienced in that point. However, the pathloss $\overline{PL}(\text{dB})$ in (6) is a function of a UAV's altitude h_i and its horizontal distance to the ground user r_i. Hence, for a fixed hovering altitude h_i, all the ground users at the radial distance r_i experience the same pathloss. It is equivalent to saying that the locus of the points on the 2D area that experience the same pathloss is a circle centered at the ground image of the UAV. Thus, the coverage region of a UAV-BS is a circular disk. ■

We define the coverage radius for a UAV-BS U_i with transmit power P_i^t as the radial distance in which the received signal power on a ground receiver reaches the threshold ϵ, i.e.,

$$R_i \triangleq r_i|_{\overline{PL}(\text{dB}) = P_i^t(\text{dB}) - \epsilon}, \quad (9)$$

in which R_i is the coverage radius of UAV-BS U_i. Using (6), the above condition can be re-written as:

$$20\log(d_i) + \frac{A}{1 + \alpha \exp(-\beta(\arctan\big(\frac{h_i}{R_i}\big) - \alpha))} + B + \epsilon - P_i^t = 0, \quad (10)$$

where $d_i = \sqrt{h_i^2 + R_i^2}$. The equation in (10) shows that R_i is an implicit function of h_i. However, as it is shown in [19], the equation in (10) is a unimodal function and has only one stationary point which corresponds to the maximum coverage radius. Let h_i^* denote the optimal flight altitude which results in the maximum coverage radius. We find h_i^* by taking partial derivative from the expression in (10) as:

$$\frac{\partial R_i}{\partial h_i} = 0, \quad (11)$$

which yields the following equation:

$$\frac{h_i}{R_i} + \frac{9\ln(10)\alpha\beta A \exp\Big(-\beta[\arctan\big(\frac{h_i}{R_i}\big) - \alpha]\Big)}{\pi\Big[\alpha \exp\Big(-\beta[\arctan\big(\frac{h_i}{R_i}\big) - \alpha]\Big) + 1\Big]^2} = 0. \quad (12)$$

Numerically solving the equations in (10) and (12) gives us the optimal flight altitude h_i^* and the corresponding coverage radius R_i of the UAV-BS $U_i \in \mathcal{U}$ as a function of its transmit power P_i^t and environmental parameters.

Having found the optimal flight altitude and coverage radii for the available UAVs in the repository, we assign a profile $\mathbf{P}$ to each UAV as a tuple containing its transmit power, flight altitude, and coverage radius:

$$\mathbf{P_i} \triangleq (P_i^t, h_i^*, R_i), \quad i = 1, \ldots, N. \quad (13)$$

Next, we discuss the problem of optimal resource allocation (selection of UAVs) and the horizontal placement of the UAV-BSs.

IV. OPTIMAL SELECTION AND HORIZONTAL PLACEMENT OF UAVS

In this section, we investigate the joint problem of resource allocation and coverage maximization for a heterogeneous set of UAVs. Given a 2D area on the ground, our aim is to

select the best subset of the available UAVs to provide wireless coverage in the area with minimal energy consumption. Furthermore, we want to optimize the 2D location of the UAVs in the horizontal plane in order to maximize the total coverage while avoiding interference. To provide the maximum coverage in a geographical region with minimum total transmit power, one needs to answer the following questions:

- How many and which types of the UAVs should be deployed to provide maximum coverage?
- What is the optimal placement of UAVs?

These questions can be formulated as the following optimization problem:

$$\underset{I_i,x_i,y_i}{\text{maximize}} \quad \sum_{i=1}^{N} I_i \left(\pi R_i^2 - \vartheta P_i^t\right), \tag{14}$$

$$\text{s.t. } I_i \in \{0,1\}, \quad i \in \{1,2,\cdots,N\} \tag{15}$$

$$-\frac{W}{2}+R_i \le x_i \le \frac{W}{2}-R_i, \quad i \in \{1,2,\cdots,N\}|I_i=1 \tag{16}$$

$$-\frac{L}{2}+R_i \le y_i \le \frac{L}{2}-R_i, \quad i \in \{1,2,\cdots,N\}|I_i=1 \tag{17}$$

$$\sqrt{(x_i-x_j)^2+(y_i-y_j)^2} \ge R_i+R_j, \quad i,j \in \{1,2,\cdots,N\}|i\neq j, \quad I_i=I_j=1. \tag{18}$$

where N is the total number of available UAVs in the repository. In addition, I_i is an indicator function which equals to 1 if UAV $U_i \in \mathcal{U}$ is selected for covering the region and equals to 0 otherwise. It governs the resource allocation strategy for a given area of interest. Moreover, in (14), ϑ is the weighting factor, where setting $\vartheta = 0$ results in coverage maximization problem without considering energy efficiency. The objective function in (14) makes a trade-off between the covered area and the total transmission power. The constraint in (15) states that the indicator function can only take on 0 and 1 while constraints in (16) and (17) ensure that the coverage circle of UAV U_i with radius R_i does not extend outside the rectangle, thereby prevents its transmission to be wasted covering outside of the desired area. Finally, the constraint in (18) avoids overlap between the cells to reduce the risk of interference between the cells.

Due to its non-convexity, non-linear constraints, and a high number of unknowns, the optimization problem stated in (14)-(18) is very challenging to solve. However, it has an analogy with the so called *circle packing (CP) problem* [29]. In the CP problem, the task is to arrange a given number of circles, say K circles, on a surface such that no overlapping occurs. The goal is to maximize the packing density, which is defined as the proportion of the surface covered by the circles. The problem is known to be NP-hard [29], and hence, there does not exist a polynomial time algorithm to solve it optimally. There are some studies in the literature to tackle the CP problem, most of which focus on packing equal circles into a container and are heavily influenced by the congruence of the circles. Nevertheless, the optimization problem in (14) has three distinctive differences with the CP problem which mandate devising a solution tailored to the specific properties of the problem in hand:

1) Unlike the CP problem, which primarily aims at maximizing the coverage, in the formulated problem in (14), in addition to the coverage maximization, there is a penalty term ϑ which assigns a price, i.e., transmit power, to a circle, i.e., UAV-BS' coverage disk, which is to be minimized;
2) Different from the CP problem, the number of coverage circles are not known a priori. In fact, the indicator function $I_i|_{i=1}^{N}$ determines whether a coverage circle is used to pack the desired surface or not;
3) In contrast to the CP problem, the radii of the coverage circles are predetermined and fixed as they are a function of the UAV-BS' transmit power.

Next, we propose a novel algorithm to solve the problem stated in (14)-(18).

V. PROPOSED ALGORITHM

In order to solve the optimization problem in (14)-(18), we develop an evolutionary-based approach which finds the best strategy for arranging the coverage circles in the desired 2D surface. For this purpose, we first develop a novel algorithm called Maximal Density Positioning (MDP) to pack an ordered set of the coverage circles into the rectangular surface satisfying the non-overlapping and maximal density conditions. Then, we propose an evolutionary algorithm to intelligently search through the feasible arrangements found by the MDP algorithm to find the solution which results in the highest utility according to the objective function presented in (14).

A. MAXIMAL DENSITY POSITIONING (MDP)

Given the N circles with various radii, there are $N!$ possible ways of storing their radii in an ordered N-tuple. Let $\mathcal{R} = \{R_1, R_2, \ldots, R_N\}$ denote the set of all coverage circles and $\phi : \mathcal{R} \mapsto \mathcal{R}$ is a permutation over the set $\mathcal{R}$ which is a bijection function from $\mathcal{R}$ to itself,

$$\phi = \left[\phi(R_1), \phi(R_2), \ldots, \phi(R_N)\right]. \tag{19}$$

For instance, a particular permutation of the set $\{R_1, R_2, R_3\}$ can be written as: $\phi = \left[R_2, R_3, R_1\right]$, in which $\phi(R_1) = R_2$, $\phi(R_2) = R_3$, and $\phi(R_3) = R_1$. We denote the set of all permutations of the set $\mathcal{R}$ with $\Delta = \{\phi_1, \phi_2, \ldots, \phi_{N!}\}$.

Given a particular permutation ϕ_k, we aim at placing the coverage circles in the rectangular surface so that the arrangements satisfies the following conditions:

- Circles must be placed in the rectangular surface in the order of their indices, starting from index 1;
- Circles must be completely inside the rectangle based on the constraints in (16) and (17);
- Circles should not overlap with one another according to constraint in (18);

- To acquire the maximum packing density, circles should be tangent either to other circles in the rectangle or the rectangle borders.

Let $[-\frac{W}{2}, -\frac{L}{2}]$, $[\frac{W}{2}, -\frac{L}{2}]$, $[\frac{W}{2}, \frac{L}{2}]$, and $[-\frac{W}{2}, \frac{L}{2}]$ be the coordinates of the rectangular area in the 2D Cartesian plane. Given an ordered tuple of circles ϕ_k, the Maximal Density Positioning (MDP) algorithm finds a feasible solution for the optimization problem in (14)-(18). Before proceeding with the procedure of MDP, we first need to define the locus of the center for a circle as follows.

Definition 1: Consider a rectangle with length L and width W within which there exists a set of circles $\mathcal{C}$ satisfying the conditions stated in (16), (17), and (18). The *locus of the center* (LoC_i) for a circle with radius R_i is the set of all points (x_i, y_i) at which its center can be placed while all the conditions in (16), (17), and (18) are still satisfied. Formally,

$$\begin{aligned}\text{LoC}_i = \{(x_i, y_i) \big| \; & | \, x_i \, | \leq | \, \frac{W}{2} - R_i \, |, \\ & | \, y_i \, | \leq | \, \frac{L}{2} - R_i \, |, \\ & \sqrt{(x_i - x_j)^2 + (y_i - y_j)^2} \geq R_i + R_j, \\ & \forall j \in \mathcal{C}, I_j = 1\}. \end{aligned} \tag{20}$$

Given a particular permutation ϕ, MDP finds the LoC_1 for the first circle with radius $\phi(R_1)$ which is a smaller rectangle inside the rectangular surface with its edges having a distance $\phi(R_1)$ from the boundaries, as shown in Figure. 2.a. If LoC_1 is not an empty set, it then places the the center of the first circle on the lower left-most corner of the LoC_1 and flags its corresponding indicator function, as shown in Figure. 2.b. If the LoC_1 is empty, it assigns 0 to the corresponding indicator function, removes the circle R_1 from the list, and proceeds to the next circle in ϕ_k. Having already placed k circles in the desired surface, for the $(k+1)$th circle with radius R_{k+1}, it first computes its LoC_{k+1}. Then, if $\text{LoC}_{k+1} \neq \emptyset$, it selects the lower left-most point on the LoC_{k+1} to place the circle. If the locus is empty, i.e., $\text{LoC}_{k+1} = \emptyset$, then it is not possible to insert the circle according to the mentioned constraints. Consequently, it removes all the remaining circles with the same size from the ordered tuple ϕ and proceeds to the next circle in the list. It stops when there are no more circles remaining in the list. Finally, the MDP algorithm produces two subsets of ϕ: (a) a subset S of the circles that are placed into the area, and (b) a subset U of the circles that cannot be fitted in the area. Figure 2 illustrates an example of MDP when packing a tuple of two circles with radii $\phi = [2, 1]$ in a 10×10 square. Algorithm 1 shows the pseudocode for the proposed MDP algorithm.

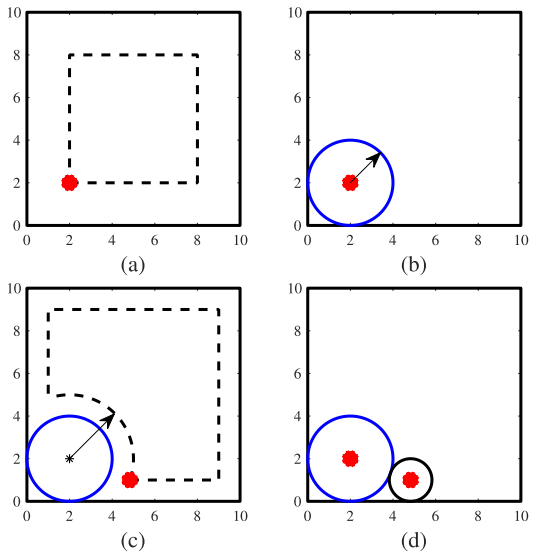

FIGURE 2. An illustration of MDP algorithm for packing two circles with radii 2 and 1 in a 10 × 10 square: (a) the LoC for the first circle with radius 2. The red point shows the lower left-most corner on the locus. (b) The first circle in packed in the square. (c) The LoC for the second circle with radius 1. (d) Both circles are placed in the square. They are tangent to one another and the square's edges.

Algorithm 1 Maximal Density Positioning (MDP)

Data: $\Phi = [\phi(R_1), \phi(R_2), \ldots, \phi(R_N)]$ and the dimensions of rectangle $[W, L]$
Result: A feasible solution to the optimization problem in (14)-(18)

Initialization: $S \leftarrow \emptyset$ and $U \leftarrow \emptyset$
for $i \leftarrow 1$ **to** N **do**
  if $\phi(R_i) \notin U$ **then**
    Compute LoC_i
    if $\text{LoC}_i \neq \emptyset$ **then**
      Find (a_i, b_i), the lower leftmost point on LoC_i
      $(x_i, y_i) \leftarrow (a_i, b_i)$
      $I_i \leftarrow 1$
      Append $\phi(R_i)$ to S
    else
      for $j \leftarrow i$ **to** N **do**
        if $\phi(R_j) = \phi(R_i)$ **then**
          Append $\phi(R_j)$ to U
          $I_j \leftarrow 0$
        end
      end
    end
  else
    continue
  end
end
return S *and* U

Proposition 2: The MDP algorithm yields a 2D arrangement of the coverage circles inside the desired area which is a feasible solution to the optimization problem expressed in (14)-(18).

Proof: By construction, given an ordered list of circles Φ, the MDP algorithm places a circle with radius R_i inside the rectangle if and only if $\text{LoC}_i \neq \emptyset$. According to Definition 1, if there exists a point $(x_i, y_i) \in \text{LoC}_i$, then placing the center of R_i at (x_i, y_i) does not violate the constraints

in (16), (17), and (18), and thus, the arrangement is a feasible solution to the optimization problem in (14). ■

Complexity Analysis: The overall complexity of the MDP algorithm mainly depends on calculating LoC_i, i.e., the locus of center for circle $\phi(R_i)$, in line 4 of Algorithm 1. For $i = 1$, the computation of LoC_1 is trivial as shown in Figure 2. However, for $i \geq 2$, the computation of LoC_i requires solving at most $\binom{i-1}{2} + 4(i-1)$ quadratic equations. To see this, assume that there are already $i-1$ circles placed in the rectangle. In order to prevent any overlap between $\phi(R_i)$ and the first circle in the rectangle with radius $\phi(R_1)$, the LoC_i should not contain any points within the circle with radius $\phi(R_1) + \phi(R_i)$. The same reasoning applies to all the other circles which are already placed in the rectangle. Thus, to compute the LoC_i, we need to find the intersection points between $i-1$ circles with radii $\{\phi(R_1) + \phi(R_i), \phi(R_2) + \phi(R_i), \ldots \phi(R_{i-1}) + \phi(R_i)\}$. Computing the intersection points of $i-1$ circles requires solving $\binom{i-1}{2}$ quadratic equations. Moreover, to ensure that $\phi(R_i)$ is inside the rectangle, i.e., satisfying the boundary conditions in (16) and (17), we need to compute the intersection points of the mentioned circles with the horizontal and vertical lines $x = -\frac{W}{2} + \phi(R_i)$, $x = \frac{W}{2} - \phi(R_i)$, $y = -\frac{L}{2} + \phi(R_i)$, and $y = \frac{L}{2} - \phi(R_i)$, which requires solving $4 \times (i-1)$ quadratic equations. Therefore, we need to solve $\binom{i-1}{2} + 4(i-1)$ quadratic equations to find the intersection points in iteration i. Next, we need to check if there exist some intersection points that are not within any of the mentioned circles. In the worst case scenario that every two circles intersect at two points, we have $2\binom{i-1}{2}$ intersection points and since there are $(i-1)$ circles, we need to check $2(i-1)\binom{i-1}{2}$ conditions. Therefore, the total number of operations for computing the LoC_i in iteration i is equal to $(2i-1)\binom{i-1}{2} + 4(i-1)$.

Having computed LoC_i, if $\text{LoC}_i \neq \emptyset$ we select the lower leftmost intersection point as the center of $\phi(R_i)$ and proceed to the next circle in the list (lines 5 to 9 of Algorithm 1). However, if $\text{LoC}_i = \emptyset$, we add the circle $\phi(R_i)$ and all the remaining circles with the same radius to the list U in order to prevent repeated calculations for similar circles that cannot be fitted into the rectangle (lines 11 to 16 of Algorithm 1). In the worst case scenario, we have $\text{LoC}_i \neq \emptyset$ for all i. Therefore, in the worst case scenario, lines 11 to 16 of Algorithm 1 will not be executed, and instead, the algorithm calculates LoC_i for all circles, as stated in lines 5 to 10. In addition to finding LoC_i, there are two "assignment" functions in lines 7 and 8 and an "append" function in line 9 which are of $\mathcal{O}(1)$ complexity. Moreover, the "find" function in line 6 is of linear complexity over a list of $2\binom{i-1}{2}$ intersection points. Thus, the lines 5 to 10 require $2\binom{i-1}{2} + 3$ operations in each iteration. The total number of operations is given by:

$$\sum_{i=2}^{N} \left[(2i+1)\binom{i-1}{2} + 4i - 1\right] = \sum_{i=2}^{N} \left[i^3 - \frac{5}{2}i^2 + \frac{9}{2}i\right] = \frac{1}{4}N^4 + g(N), \quad (21)$$

where $g(N)$ is a polynomial of degree 3. Thus, assuming that the quadratic equations can be solved in constant time, the complexity of the MDP problem can be written as $\mathcal{O}(N^4)$. It can be seen that the MDP algorithm has a polynomial time complexity which translates into a good scalability.

Using MDP, we can find all the feasible solutions for the optimization problem stated in (14)-(18) and then find the best solution which maximizes the objective function through exhaustive search. However, computing all the feasible solutions is computationally expensive. In the next section, we propose a evolutionary-based algorithm which uses only a fraction of the feasible solutions to find the optimal solution of the problem.

B. THE BEST FEASIBLE SOLUTION

To find the *optimal solution*, one can search over all feasible solutions and check which one maximizes the objective function in (14). However, as the number of UAVs increases, the input size, i.e., the number of feasible solutions, grows in factorial time. Thus, the exhaustive search method is not a practical solution. In this section, we propose a more effective evolutionary-based algorithm to find the optimal solution of optimization problem in (14). As discussed in the previous section, for any permutation ϕ of the available coverage circles, the MDP algorithm partitions ϕ into two mutually exclusive subsets S and U corresponding to the fitted coverage circles and left-out coverage circles, respectively. Let $X \| Y$ denote the concatenation of two ordered lists X and Y. Adopting the terminology of Genetic Algorithm [30], we define a *candidate solution* as follows:

Definition 2: For any permutation $\phi_k \in \Delta, k = 1, \ldots, N!$, a candidate solution $\Psi_k \triangleq S_k \| U_k$ is defined as the concatenation of (i) a feasible solution S_k to the optimization problem, and (ii) a set $U_k = \phi_k \setminus U_k$ of the circles that cannot be positioned inside the area of interest. Each item, i.e., coverage circle, in the candidate solution ϕ_k is called an *individual*.

The order of an individual in the candidate solution is the order in which it is considered by the MDP algorithm. Each candidate solution Ψ_k corresponds to a unique layout in which the first $|S_k|$ individuals constitute a feasible solution to (14), where $|S_k|$ denotes the cardinality of the list S_k.

Since the objective of the optimization problem in (14)-(18) is to maximize the coverage area while minimizing the total power transmit using the available UAVs, we define the following *utility* function for each candidate solution:

$$\Pi(\Psi_k) = \sum_{i=1}^{|S_k|} \pi R_i^2 - \vartheta P_i^t \quad (22)$$

in which $|S_k|$ is the number of coverage circles in the feasible solution S_k while the R_i and P_i^t represent the corresponding coverage radius and transmit power, respectively.

To intelligently search through the space of feasible solutions, we first generate a set of candidate solutions and then, by introducing some dynamic rules we let the candidate

solutions evolve toward achieving higher utility values. Consider a set of $K < N!$ permutations $\phi_1, \phi_2, \ldots, \phi_K$ of the set $\mathcal{R}$, where K is the *population size*. Using the MDP algorithm, we transform these permutations to candidate solutions. Let $\Upsilon = \{\Psi_1, \Psi_2, \ldots, \Psi_K\}$ denote the set of candidate solutions. At each time step t, the set of candidate solutions Υ^t evolves in order to contain candidate solutions with higher utility.

Definition 3: For each candidate solution Ψ_k, $k = 1, 2, \ldots, K$, the *selection probability* is defined as the relative utility of Ψ_k compared to the whole set of candidate solutions:

$$\Pr(\Psi_k) = \frac{\Pi(\Psi_k)}{\sum_{i=1}^{K} \Pi(\Psi_i)}. \tag{23}$$

Note that $\Pr(\Psi_k) \geq 0$ and $\sum_{k=1}^{K} \Pr(\Psi_k) = 1$. Thus, the equation in (23) defines a probability distribution over the set of candidate solutions Υ.

Consider parameter $0 < \mu < 1$ as a design factor which determines what percentage of the current population will move to the next population set unchanged. Assume that $(1 - \mu) \times K$ candidate solutions in Υ^t will be randomly selected according to the probability distribution in (23) and transferred to the next set of candidate solution Υ^{t+1}. Since the probability distribution in (23) assigns a higher selection probability to the candidate solutions with higher utility, Υ^{t+1} is expected to contain *better* candidate solutions compared to Υ^t. The remaining $\mu \times K$ candidate solutions in Υ^t will be evolved based on the following dynamic rules:

- **Crossover**: In the remaining $\mu \times K$ candidate solutions, we randomly select $\frac{\mu \times K}{2}$ pairs of candidate solutions according to (23). Let Ψ_i^t and Ψ_j^t be a pair of candidate solutions in time step t. Let a and b be two randomly selected integers such that $1 \leq a < b \leq N$. Considering two indices a and b, the candidate solution Ψ_i^{t+1} inherit a subsequence $[a, \ldots, b]$ of its individuals from Ψ_i^t. The individuals of Ψ_j^t are then used in their order of appearance to successively fill the remaining empty indices of Ψ_i^{t+1}. If an individual of Ψ_j^t is already in Ψ_i^{t+1}, it is rejected, else it is positioned in the first empty index of Ψ_i^{t+1}. A similar procedure is applied to compose Ψ_j^{t+1} from Ψ_i^t and Ψ_j^t.
- **Mutation**: To increase the diversity of the solution set in each time step, we assume that the candidate solutions Ψ_i^t, $i = 1, 2, \ldots, K$, are subject to a process of mutation with small probability ξ in which, two randomly selected individuals of Ψ_i^t are swapped to create Ψ_i^{t+1}.

In each time step t, the feasible solution with the highest utility value is denoted by Ψ^{t*}. The procedures of evaluation, selection, and reproduction are repeated until the utilities of best feasible solutions in two consecutive iterations are within a small distance δ of each other, i.e., $|\Pi(\Psi^{t*}) - \Pi(\Psi^{t+1*})| \leq \delta$, or the maximum number of iterations is reached. The maximum number of iterations is denoted by T. Note that small values of δ results in more accurate answer with possibly a greater number of required iterations. Algorithm 2 shows the pseudocode for the proposed evolutionary algorithm.

Complexity Analysis and Convergence: In order to find the time complexity of the proposed evolutionary algorithm, we first need to characterize the complexity of the crossover and mutation operators. As shown in [31], the time complexity of partially mapped crossover operation for a list of N elements is $\mathcal{O}(N)$. Furthermore, as the mutation operator involves swapping two elements in a N-tuple, its time complexity is also $\mathcal{O}(N)$ [32]. Let $c_1 N$ and $c_2 N$ denote the number of "constant-time" operations required by the crossover and the mutation operators, respectively, where c_1 and c_2 are positive real numbers. Note that as the asymptotic time complexity is concerned, the lower order terms are dropped.

The proposed evolutionary algorithm is composed of two main stages. Given a population of K candidate solutions, in each iteration, it first computes the utility of each candidate solution according to the utility function in (22), and selects the solution with the maximum utility as a potential output (Lines 3 to 6 of Algorithm 2). Note that computing the utility function in (22) for a list of N circles requires $4N$ arithmetic operations. Next, it generates a new population of candidate solutions evolved from the current population (Lines 8 to 21 of Algorithm 2). Since the first stage involves the computation of utility function (22) for a population of size K, it requires $c_3 KN$ constant-time operations in which c_3 is a positive real number. The second stage mainly involves performing the crossover and mutation over the population of size K of N-tuples which requires $c_1 KN$ and $c_2 KN$ operations, respectively. Furthermore, similar to the first stage, it requires the utility function in (22) to be evaluated for the newly generated population which needs $c_3 KN$ operations. In conclusion, each iteration of Algorithm 2 requires performing $c_1 KN + c_2 KN + 2c_3 KN$ constant-time operations. Since the maximum number of iterations is equal to T, in the worst case scenario, Algorithm 2 requires $(c_1 + c_2 + 2c_3)KNT$ operations. Therefore, the complexity of Algorithm 2 can be written as $\mathcal{O}(KNT)$. Note that both the population size K and the maximum number of iterations T are design factors with a linear effect on the time complexity of the algorithm. Thus, they can be adjusted to meet the desired trade-off between the solution accuracy and the time complexity of the algorithm.

The convergence of Algorithm 2 is guaranteed by the parameter T which determines the maximum number of allowed iterations. As specified in line 2 of Algorithm 2, the proposed algorithm may converge before reaching T iterations if $|\Pi(\Psi^t) - \Pi(\Psi^{t+1})| \leq \delta$, which means that two consecutive generations of candidate solutions produce roughly the same utility.

VI. SIMULATION RESULTS

For simulations, we consider the UAV-based communications over 2 GHz carrier frequency, i.e., $f_c = 2$ GHz, in an urban environment with parameters $\alpha = 9.61$, $\beta = 0.16$, and $(\eta_{LoS}, \eta_{NLoS}) = (1 \text{ dB}, 20 \text{ dB})$ [9]. We assume that the minimum allowable received signal power for a successful transmission is $\epsilon = -60$ dBm. We also consider a repository of 16 UAVs in which there are four different types of UAVs

Algorithm 2 Proposed evolutionary algorithm to find the best feasible solution to (14)-(18)

Data: $\Upsilon = \{\Psi_1, \Psi_2, \ldots, \Psi_K\}$, μ, ξ, δ, T
Result: Ψ^*, Π^*
Initialization: $t \leftarrow 0, \quad \Pi \leftarrow 0, \quad \Upsilon^t \leftarrow \Upsilon$
while $|\Pi(\Psi^t) - \Pi(\Psi^{t+1})| > \delta$ **or** $t \leq T$ **do**
  forall the $\Psi_i \in \Upsilon^t$ **do**
    Compute the utility $\Pi(\Psi_i)$ according to (22)
  end
  $\Pi(\Psi^t) \leftarrow \max(\Pi(\Psi_i))\big|_{i=1}^{K}$
  # **Create generation** $t+1$ **of candidate solutions:**
  Select $(1-\mu) \times K$ members of Υ^t according to (23) and insert them into Υ^{t+1};
  Select $\mu \times K$ members of Υ^t according to (23); pair them up; perform crossover; insert the resulting candidate solutions to Υ^{t+1};
  forall the $\Psi_j \in \Upsilon^{t+1}$ **do**
    Select a random number q in range [0, 1];
    if $q \leq \xi$ **then**
      Select two random individuals in Ψ_j and swap their positions;
    end
  end
  forall the $\Psi_j \in \Upsilon^{t+1}$ **do**
    Compute the utility $\Pi(\Psi_j)$ according to (22)
  end
  $\Pi(\Psi^{t+1}) \leftarrow \max(\Pi(\Psi_j))\big|_{j=1}^{K}$
  $t \leftarrow t+1$
end
return *The feasible solution* Ψ^* *with the highest utility value*

with transmit powers of 35 dBm, 39 dBm, 43 dBm, and 50 dBm and there are four identical UAVs of each kind. The goal is to provide wireless coverage for a 10 Km $\times$ 10 Km area. The simulation parameters are summarized in Table 1.

TABLE 1. Simulation parameters.

Parameter	Value	Parameter	Value	Parameter	Value
α	9.61	f_c	2 GHz	W	10 Km
β	0.16	ϵ	-60 dBm	ϑ	0.01
η_{LoS}	1 dB	L	10 Km	N	16
η_{NLoS}	20 dB	K	300	δ	0.01
T	1000	μ	0.5	ξ	0.05
$P^t \in \{35\text{dBm}, 39\text{dBm}, 43\text{dBm}, 50\text{dBm}\}$					

Note that for this scenario, we have approximately $\frac{16!}{4!4!4!4!} \approx 6.3 \times 10^7$ unique permutations. Using an exhaustive search method, we have to check the utility of each and every one of these permutations by the MDP algorithm to find the best solution. However, using the proposed evolutionary algorithm, we consider a population size of only 300 unique permutations and we run a Monte Carlo simulation of 100 times to smooth out the randomness effect of the population selection.

Figure 3 shows the optimal flight altitude along with the maximum coverage radius as a function of transmit power by numerically solving equations (10) and (12), simultaneously. As it is seen in Figure 3, by increasing the transmit power, both the optimal flight altitude and the maximum coverage radius will increase with a similar rate. It is observed that for large values of P^t, the optimal altitude may exceed beyond the physical constraints for LAP systems which requires imposing a constraint on h for practical scenarios. Moreover, using Figure 3, we can obtain the profile of the UAVs as

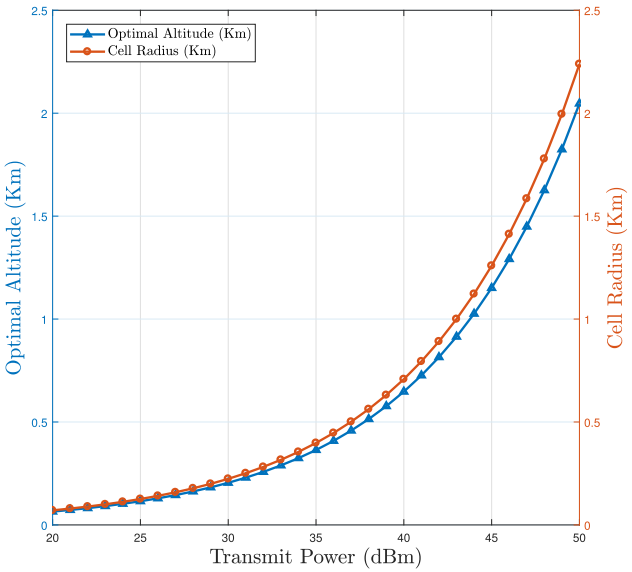

FIGURE 3. Optimal flight altitude and the corresponding cell radius for UAV-BSs with various transmit power in an urban environment.

defined in (13). Since there are four different types of UAV in the repository, we have four distinctive UAV profiles: $\mathbf{P_1}$ = (35 dBm, 0.36 Km, 0.4 Km), $\mathbf{P_2}$ = (39 dBm, 0.57 Km, 0.64 Km), $\mathbf{P_3}$ = (43 dBm, 0.91 Km, 1 Km), and $\mathbf{P_4}$ = (50 dBm, 2.04 Km, 2.41 Km), in which the first, second, and third element refer to their transmit power, optimal flight altitude, and coverage radius, respectively.

Figure 4 illustrates the optimal resource allocation and 3D placement of the UAVs for providing maximum coverage without inter-cell interference in the area of interest. It can be seen that only 13 UAVs out of the 16 available UAVs are deployed in the area since deploying more UAVs would unavoidably cause an interference. Indeed, only a single UAV with transmit power 43 dBm is employed while the UAVs in other groups are all utilized.

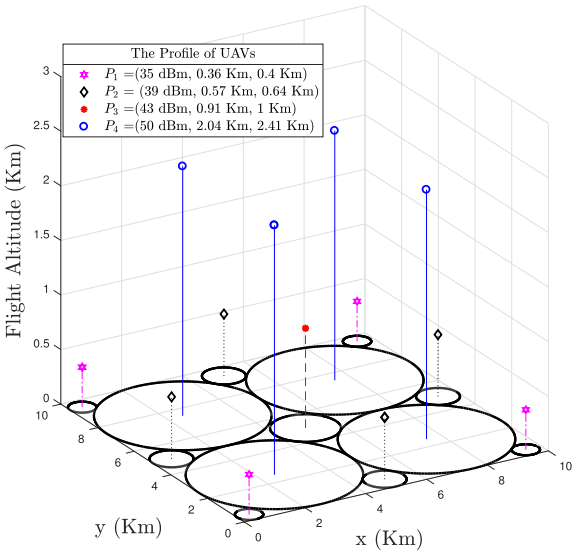

FIGURE 4. The optimal 3D placement of the UAVs for maximum coverage area while avoiding inter-cell interference.

Depends on the size and shape of the area of interest as well as the properties of available UAVs. The optimal deployment in Figure 4 yields 88.52% coverage percentage in the area.

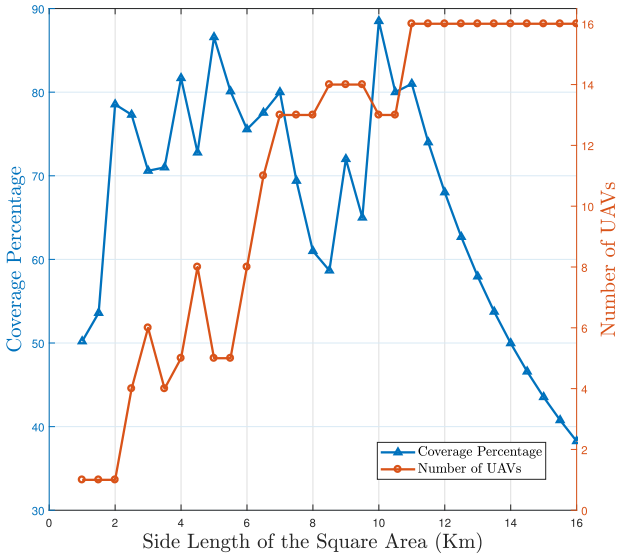

FIGURE 5. The coverage percentage and the number of deployed UAVs for different network sizes.

Figure 5 shows the coverage percentage and the number of deployed UAVs as a function of the network size for a square area. Clearly, the number of deployed UAVs is not a monotonically increasing function of the size of the area. This is due to the heterogeneity of the UAVs and the disparity between their coverage radii. Interestingly, based on the available UAVs in the repository, the maximum coverage percentage is achieved for a 10 Km × 10 Km area using only 13 UAVs. However, as the side length of the area increases to 11 Km, all the 16 UAVs can be deployed without any inter-cell interference. Therefore, increasing the side length beyond 11 Km accentuates the resource deficiency as the coverage percentage monotonically decreases. The type of deployed UAVs along with their optimal placement is shown in Table 2. For example, for a 3 Km × 3 Km area, a total of 6 UAVs are deployed in which 4 UAVs are of the same type with profile $\mathbf{P_1}$ are placed at the horizontal locations (2.26 Km, 0.4 Km), (0.4 Km, 2.26 Km), (2.43 Km, 1.18 Km), and (1.18 Km, 2.43 Km). Furthermore, a single UAV with

TABLE 2. Horizontal location of the UAVs.

UAV Profile	Length of The Area: 1 Km	3 Km	5 Km	7 Km	9 Km	11 Km
$\mathbf{P_1}$ = (35 dBm, 0.36 Km, 0.4 Km)	(0.4, 0.4)	(2.26, 0.4) (0.4, 2.26) (2.43, 1.18) (1.18, 2.43)	(0.4, 0.4) (4.37, 0.4) (0.4, 4.37) (4.37, 4.37)	(o.4, 0.4) (3.85, 4.82) (5.44, 5.20) (4.54, 5.22)	(0.4, 0.4) (7.71, 7.90) (1.37, 7.90) (7.90, 1.59)	(0.4, 0.4) (4.37, 0.4) (0.4, 4.37) (5.26, 0.4)
$\mathbf{P_2}$ = (39 dBm, 0.57 Km, 0.64 Km)	-	(2.19, 2.19)	-	(6.26, 4.56) (4.56, 6.26) (6.26, 5.48) (4.58, 4.22)	(7.11, 0.64) (0.64, 7.11) (2.72, 5.44) (5.42, 2.85)	(9.71, 0.64) (0.64, 9.71) (10.36, 1.74) (1.74, 10.36)
$\mathbf{P_3}$ = (43 dBm, 0.91 Km, 1 Km)	-	(1, 1)	-	(1, 5.51) (5.51, 1) (5.90, 2.96) (2.96, 5.90)	(5.51, 1) (1, 5.51) (2.64, 7.30) (7.30, 2.85)	(4.82, 4.82) (4.82, 9.64) (9.64, 4.82) (9.64, 9.64)
$\mathbf{P_4}$ = (50 dBm, 2.04 Km, 2.41 Km)	-	-	(2.41, 2.41)	(2.41, 2.41)	(2.41, 2.41) (5.74, 5.89)	(2.41, 2.41) (7.23, 2.41) (2.41, 7.23) (7.23, 7.23)

profile $\mathbf{P_2}$ and one UAV with profile $\mathbf{P_3}$ are also deployed at the horizontal locations (2.19 Km, 2.19 Km) and (1 Km, 1 Km), respectively. This arrangement of the UAVs is the optimal arrangement satisfying the constraints in (15)-(18) and yields 71.54% coverage area.

Figure 6 shows the total power usage by the UAV-BSs as a function of the size of the area for two different values of the weighting factor ϑ in (14). It can be seen that as the size of the region of interest increases, the required total transmission power will increase as well in order to cover the area. As mentioned before, setting $\vartheta = 0$ is equivalent to maximizing the total coverage area by the UAVs without considering the energy efficiency. However, by increasing ϑ from 0 to 0.02, the power consumption noticeably decreases. This is due to the fact that increasing ϑ favors deploying UAVs with smaller transmit power according to the utility function in (22). However, smaller transmit power results in smaller coverage radius as well. Therefore, the weighting factor ϑ captures the trade-off between the power consumption and the desired coverage percentage which depends on the shape and size of the area as well as the characteristics of the available resources in the repository.

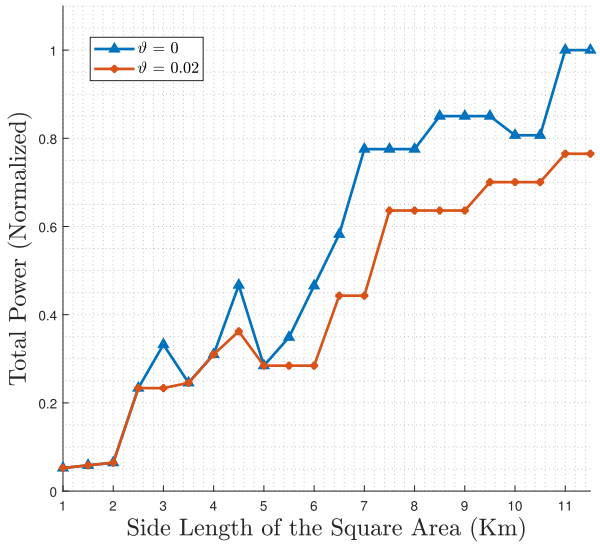

FIGURE 6. Total power consumption versus the size of the area for different values of weighting factor ϑ.

VII. CONCLUSION

This paper developed an effective method for resource allocation and optimal 3D placement of a set of heterogeneous UAVs acting as flying base stations to provide wireless coverage for ground users in an area. First, we derived the optimal flight altitude of the UAVs as a function of their transmit power and environmental parameters. Then, to provide the maximum wireless coverage with the available UAVs, we formulated an optimization problem which jointly determines the optimal resource allocation strategy along with the location of the UAVs. The problem is known to be NP-hard, for which we proposed a novel algorithm to solve the optimization problem. The proposed algorithm is composed of two modules. The first module, i.e., the (MDP) algorithm, finds the set of all feasible solutions to the optimization problem. The second module exploits an evolutionary algorithm to intelligently search through the set of feasible solutions and find the best arrangement of the UAVs for maximum coverage. Finally, simulation results are provided, which show the effectiveness of the developed 3D cell-planning and performance of the proposed algorithm.

ACKNOWLEDGMENT

The U.S. Government is authorized to reproduce and distribute reprints for Governmental purposes notwithstanding any copyright notation thereon. The views and conclusions contained herein are those of the authors and should not be interpreted as necessarily representing the official policies or endorsements, either expressed or implied, of Air Force Research Laboratory, OSD, or the U.S. Government.

REFERENCES

[1] Y. Zeng, R. Zhang, and T. J. Lim, "Wireless communications with unmanned aerial vehicles: Opportunities and challenges," *IEEE Commun. Mag.*, vol. 54, no. 5, pp. 36–42, May 2016.
[2] J.-J. Wang, C.-X. Jiang, Z. Han, Y. Ren, R. G. Maunder, and L. Hanzo, "Taking drones to the next level: Cooperative distributed unmanned-aerial-vehicular networks for small and mini drones," *IEEE Veh. Technol. Mag.*, vol. 12, no. 3, pp. 73–82, Sep. 2017.
[3] W. D. Ivancic, R. J. Kerczewski, R. W. Murawski, K. Matheou, and A. N. Downey, "Flying drones beyond visual line of sight using 4g LTE: Issues and concerns," in *Proc. Integr. Commun., Navigat. Surveill. Conf.*, Apr. 2019, pp. 1–13.
[4] C. Newton. (Apr. 2017). *Facebook Takes Flight*. [Online]. Available: https://www.theverge.com/a/mark-zuckerberg-future-of-facebook/aquila-drone-internet
[5] S. Katikala, "Google project loon," *InSight: Rivier Academic J.*, vol. 10, no. 2, pp. 1–6, 2014.
[6] M. Mozaffari, W. Saad, M. Bennis, Y.-H. Nam, and M. Debbah, "A tutorial on UAVs for wireless networks: Applications, challenges, and open problems," *IEEE Commun. Surveys Tutr.*, vol. 21, no. 3, pp. 2334–2360, 3rd Quart., 2019.
[7] D. Fuller. (2016). *AT&T Detail Network Testing of Drones in Football Stadiums*. [Online]. Available: https://www.androidheadlines.com/2016/09/att-detail-network-testing-of-drones-in-football-stadiums.html
[8] A. A. Khuwaja, Y. Chen, N. Zhao, M.-S. Alouini, and P. Dobbins, "A survey of channel modeling for UAV communications," *IEEE Commun. Surveys Tutr.*, vol. 20, no. 4, pp. 2804–2821, 4th Quart., 2018.
[9] A. Al-Hourani, S. Kandeepan, and A. Jamalipour, "Modeling air-to-ground path loss for low altitude platforms in urban environments," in *Proc. IEEE Global Commun. Conf.*, Dec. 2014, pp. 2898–2904.
[10] Q. Feng, J. McGeehan, E. K. Tameh, and A. R. Nix, "Path loss models for air-to-ground radio channels in urban environments," in *Proc. IEEE Veh. Technol. Conf. (VTC)*, May 2006, pp. 2901–2905.
[11] J. Holis and P. Pechac, "Elevation dependent shadowing model for mobile communications via high altitude platforms in built-up areas," *IEEE Trans. Antennas Propag.*, vol. 56, no. 4, pp. 1078–1084, Apr. 2008.
[12] I. Bucaille, S. Héthuin, A. Munari, R. Hermenier, T. Rasheed, and S. Allsopp, "Rapidly deployable network for tactical applications: Aerial base station with opportunistic links for unattended and temporary events absolute example," in *Proc. IEEE Mil. Commun. Conf.*, Nov. 2013, pp. 1116–1120.
[13] N. H. Motlagh, M. Bagaa, and T. Taleb, "UAV-based IoT platform: A crowd surveillance use case," *IEEE Commun. Mag.*, vol. 55, no. 2, pp. 128–134, Feb. 2017.
[14] E. Semsch, M. Jakob, D. Pavlicek, and M. Pechoucek, "Autonomous UAV surveillance in complex urban environments," in *Proc. IEEE/WIC/ACM Int. Joint Conf. Web Intell. Intell. Agent Technol.*, vol. 2, Sep. 2009, pp. 82–85.

[15] R. Shakeri, M. A. Al-Garadi, A. Badawy, A. Mohamed, T. Khattab, A. Al-Ali, K. A. Harras, and M. Guizani, "Design challenges of multi-UAV systems in cyber-physical applications: A comprehensive survey, and future directions," *IEEE Commun. Surveys Tutr.*, to be published.
[16] K. Daniel and C. Wietfeld, "Using public network infrastructures for UAV remote sensing in civilian security operations," Defense Tech. Inf. Center, Tech. Univ. Dortmund, Germany, Tech. Rep., Mar. 2011.
[17] J. Wang, C. Jiang, Z. Wei, C. Pan, H. Zhang, and Y. Ren, "Joint UAV hovering altitude and power control for space-air-ground IoT networks," *IEEE Internet Things J.*, vol. 6, no. 2, pp. 1741–1753, Apr. 2019.
[18] A. A. Khuwaja, Y. Chen, N. Zhao, M.-S. Alouini, and P. Dobbins, "A survey of channel modeling for UAV communications," *IEEE Commun. Surveys Tutr.*, vol. 20, no. 4, pp. 2804–2821, 4th Quart., 2018.
[19] A. Al-Hourani, S. Kandeepan, and S. Lardner, "Optimal LAP altitude for maximum coverage," *IEEE Wireless Commun. Lett.*, vol. 3, no. 6, pp. 569–572, Dec. 2014.
[20] R. I. Bor-Yaliniz, A. El-Keyi, and H. Yanikomeroglu, "Efficient 3-D placement of an aerial base station in next generation cellular networks," in *Proc. IEEE Int. Conf. Commun.*, May 2016, pp. 1–5.
[21] M. M. Azari, F. Rosas, K.-C. Chen, and S. Pollin, "Optimal UAV positioning for terrestrial-aerial communication in presence of fading," in *Proc. IEEE Global Commun. Conf.*, Dec. 2016, pp. 1–7.
[22] X. Li, H. Yao, J. Wang, X. Xu, C. Jiang, and L. Hanzo, "A near-optimal UAV-aided radio coverage strategy for dense urban areas," *IEEE Trans. Veh. Technol.*, vol. 68, no. 9, pp. 9098–9109, Sep. 2019.
[23] M. Mozaffari, W. Saad, M. Bennis, and M. Debbah, "Drone small cells in the clouds: Design, deployment and performance analysis," in *Proc. IEEE Global Commun. Conf.*, Dec. 2015, pp. 1–6.
[24] D. Orfanus, E. P. de Freitas, and F. Eliassen, "Self-organization as a supporting paradigm for military UAV relay networks," *IEEE Commun. Lett.*, vol. 20, no. 4, pp. 804–807, Apr. 2016.
[25] J. Košmerl and A. Vilhar, "Base stations placement optimization in wireless networks for emergency communications," in *Proc. IEEE Int. Conf. Commun. Workshops*, Jun. 2014, pp. 200–205.
[26] Q. Wu, Y. Zeng, and R. Zhang, "Joint trajectory and communication design for multi-UAV enabled wireless networks," *IEEE Trans. Wireless Commun.*, vol. 17, no. 3, pp. 2109–2121, Mar. 2018.
[27] J. Lyu, Y. Zeng, R. Zhang, and T. J. Lim, "Placement optimization of UAV-mounted mobile base stations," *IEEE Commun. Lett.*, vol. 21, no. 3, pp. 604–607, Mar. 2017.
[28] M. Mozaffari, W. Saad, M. Bennis, and M. Debbah, "Efficient deployment of multiple unmanned aerial vehicles for optimal wireless coverage," *IEEE Commun. Lett.*, vol. 20, no. 8, pp. 1647–1650, Aug. 2016.
[29] K. Stephenson, *Introduction to Circle Packing: The Theory of Discrete Analytic Functions*. Cambridge, U.K.: Cambridge Univ. Press, 2005.
[30] M. Mitchell, *An Introduction to Genetic Algorithms*. Cambridge, MA, USA: MIT Press, 1998.
[31] B. Rylander, "Computational Complex. genetic algorithm," Ph.D. dissertation, Univ. Idaho, Moscow, ID, USA, Jun. 2001.
[32] T. H. Cormen, C. E. Leiserson, R. L. Rivest, and C. Stein, *Introduction to Algorithms*. Cambridge, MA, USA: MIT Press, 2009.

NIMA NAMVAR (S'14) received the B.Sc. degree in electrical engineering from the Amirkabir University of Technology, Tehran, Iran, in 2010, and the M.Sc. degree in telecommunications systems from the University of Tehran, Tehran, Iran, in 2013. He is currently pursuing the Ph.D. degree with North Carolina A&T State University, Greensboro, NC, USA. His current research interests include UAV communications, device-to- device (D2D) and machine-to-machine (M2M) communications, cognitive radio networks, the Internet of Things (IoT), and the applications of machine learning and game theory in the study of wireless networks. He was a recipient of the Outstanding Graduate Researcher Award from North Carolina A&T State University, in 2017, and also the recipient of the 2019 IEEE Wireless Telecommunications Symposium (WTS) Best Paper Award.

ABDOLLAH HOMAIFAR received the B.S. and M.S. degrees from the State University of New York at Stony Brook, in 1979 and 1980, respectively, and the Ph.D. degree from the University of Alabama, in 1987, all in electrical engineering. He is currently the NASA Langley Distinguished Chair Professor and the Duke Energy Eminent Professor with the Department of Electrical and Computer Engineering, North Carolina A&T State University (NCA&TSU). He is also the Director of the Autonomous Control and Information Technology Institute and the Testing, Evaluation, and Control of Heterogeneous Large-Scale Systems of Autonomous Vehicles (TECHLAV), NCA&TSU. His current research interests include machine learning, unmanned aerial vehicles (UAVs), testing and evaluation of autonomous vehicles, optimization, and signal processing. Through his research, he has obtained funding in excess of 30 million from various U.S. funding agencies. He has written more than 350 technical publications including book chapters and journal and conference papers. He is a member of the IEEE Control Society, Sigma Xi, Tau Beta Pi, and Eta Kapa Nu. He also serves as an Associate Editor for the *Journal of Intelligent Automation and Soft Computing*. He serves as a Reviewer for the IEEE TRANSACTIONS ON FUZZY SYSTEMS, MAN MACHINES AND CYBERNETICS, and *Neural Networks*.

ALI KARIMODDINI received the bachelor's degree in electrical and electronics engineering from the Amirkabir University of Technology, in 2003, the M.Sc. degree in instrumentation and automation engineering from the Petroleum University of Technology, in 2007, and the Ph.D. degree from the National University of Singapore. In 2012, he joined the University of Notre Dame to conduct his postdoctoral studies. He is currently an Associate Professor with the ECE Department, North Carolina A&T State University. He is also the Director of the Access Laboratory and the Deputy Director of the TECHLAV DoD Center of Excellence. His research interests include control and robotics, resilient control systems, human–machine interactions, cyber-physical systems, flight control systems, and multiagent systems. His research has been supported by different federal funding agencies and industrial partners. He is a member of AIAA, ISA, and AHS.

BEHROUZ MAHAM (S'07–M'10–SM'15) received the B.Sc. and M.Sc. degrees in electrical engineering from the University of Tehran, Tehran, Iran, in 2005 and 2007, respectively, and the Ph.D. degree from the University of Oslo, Oslo, Norway, in 2010. From September 2008 to August 2009, he was with the Department of Electrical Engineering, Stanford University, Stanford, CA, USA. He was an Assistant Professor with the School of Electrical and Computer Engineering, University of Tehran, from September 2011 to September 2015. He is currently an Associate Professor of the ECE Department, School of Engineering, Nazarbayev University (NU). He is also a TWAS-affiliate. He has more than 130 publications in major technical journals and conferences. His current research interests include wireless communication, and networking and nano-neural communication. He is an Editorial Member of the IEEE TRANSACTIONS ON COMMUNICATIONS, Elsevier's *Physical Communication*, and JohnWiley & Sons *Transactions on Emerging Telecommunications Technologies*.